Research Article

Ashis Kumar Goswami, Mourad A. M. Aboul-Soud*, Neelutpal Gogoi, Mohamed El-Shazly, John P. Giesy, Burak Tüzün, Ibrahim M. Aziz, Fahad N. Almajhdi, Hemanta Kumar Sharma*

Integrative *in silico* evaluation of the antiviral potential of terpenoids and its metal complexes derived from *Homalomena aromatica* based on main protease of SARS-CoV-2

https://doi.org/10.1515/chem-2024-0085 received February 4, 2024; accepted August 4, 2024

Abstract: Substantial research is currently conducted focusing on the development of promising antiviral drugs employing *in*

* Corresponding author: Mourad A. M. Aboul-Soud, Department of Clinical Laboratory Sciences, College of Applied Medical Sciences, King Saud University, P.O. Box 10219, Riyadh, 11433, Saudi Arabia, e-mail: maboulsoud@ksu.edu.sa

* Corresponding author: Hemanta Kumar Sharma, Department of Pharmaceutical Sciences, Faculty of Science and Engineering, Dibrugarh University, Assam, Dibrugarh, 786004, India,

e-mail: hemantasharma123@yahoo.co.in

Ashis Kumar Goswami: Department of Pharmaceutical Sciences, Faculty of Science and Engineering, Dibrugarh University, Assam, Dibrugarh, 786004, India, e-mail: rs_ashisgoswami@dibru.ac.in

Neelutpal Gogoi: National Institute of Pharmaceutical Education and Research-Guwahati, Department of Pharmaceuticals, Ministry of Chemicals and Fertilizers, Government of India, Assam, Guwahati, 781101, India, e-mail: neelutpalg@gmail.com

Mohamed El-Shazly: Pharmacognosy Department, Faculty of Pharmacy, Ain-Shams University, Organization of African Unity Street, Abassia, Cairo, 11566, Egypt, e-mail: mohamed.elshazly@pharma.asu.edu.eg John P. Giesy: Toxicology Centre, University of Saskatchewan, Saskatoon, Saskatchewan, Canada; Department of Veterinary Biomedical Sciences, University of Saskatchewan, Saskatoon, Saskatchewan, Canada; Department of Integrative Biology and Center for Integrative Toxicology, Michigan State University, East Lansing, MI, United States of America; Department of Environmental Science, Baylor University, One Bear Place #97266, Waco, TX, 76798-7266, United States of America, e-mail: John_Giesy@Baylor.edu

Burak Tüzün: Plant and Animal Production Department, Technical Sciences Vocational School of Sivas, Sivas Cumhuriyet University, Sivas, Turkey, e-mail: theburaktuzun@yahoo.com

Ibrahim M. Aziz: COVID-19 Virus Research Chair, Department of Botany and Microbiology, College of Science, King Saud University, Riyadh, 11451, Saudi Arabia, e-mail: iaziz@ksu.edu.sa

Fahad N. Almajhdi: COVID-19 Virus Research Chair, Department of Botany and Microbiology, College of Science, King Saud University, Riyadh, 11451, Saudi Arabia, e-mail: majhdi@ksu.edu.sa ORCID: Mourad A. M. Aboul-Soud 0000-0001-9395-0563

silico screening and drug repurposing strategies against SARS-CoV-2. The current study aims at identifying lead molecules targeting SARS-CoV-2 by the application of in silico and molecular dynamics (MD) approaches from phytoconstituents present in *Homalomena aromatica*. The main protease (M^{pro}) enzyme of SARS-CoV-2 is taken as the target protein to perform the docking analysis of 71 molecules reported from H. aromatica by the application of different modules of Discovery Studio 2018. Five molecules were taken as prospective leads namely dihydrocuminaldehyde, p-cymen-8-ol, cuminaldehyde, p-cymene, and cuminol. In the absence of known inhibitors, a comparative study was performed with the compounds reported in the literature and potent terpenoid-metal complexes were taken into account based on known efficacy as anti-viral molecules. After performing the docking studies with Mpro enzyme of SARS-CoV-2, it was observed that the -CDocker Energy of cuminaldehyde thiosemicarbazone was 29.152, indicating a significant affinity toward Mpro. The same was also supported by the MD study. Taken together, our results provided in silico evidence that secondary metabolites derived from H. aromatica could be employed as potent antiviral agents targeting SARS-CoV-2. Our findings warrant further validation of their in vitro and in vivo efficacies prior to their development into bona fide therapeutic agents.

Keywords: secondary metabolites, drug discovery, coronavirus, virtual screening, *Homalomena aromatica*, antiviral

1 Introduction

The first instance of pneumonia-like symptoms having unknown etiology was reported to the World Health Organization (WHO) on 31st December 2019 from Wuhan City, China [1]. Subsequently, the Chinese authorities identified this disease on 7th January 2020 as a novel coronavirus and temporarily

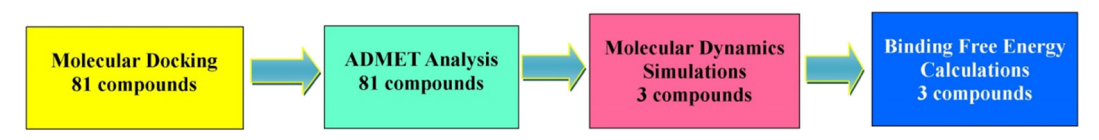
named it "2019-nCoV" [2]. On 30th January 2020, the WHO declared the outbreak as a Public Health Emergency of International Concern [3]. This infection was caused by a coronavirus that is linked to those that caused Middle East Respiratory Syndrome (MERS) in 2012 and Severe Acute Respiratory Syndrome (SARS) from 2002 to 2004. Coronaviruses (Family-Coronaviridae) in general causes respiratory and neurological diseases [4]. SARS-CoV-2 spikes (proteins protruding from the surface) bind to receptors on the human cell surface called angiotensin-converting enzyme 2. It is reported in some studies that this binding leads to infection, which is similar to the outbreak caused by the 2002 SARS outbreak [5]. Finding medications that can combat the SARS-CoV-2 virus is absolutely necessary as the world grapples with the COVID-19 outbreak [6]. Even though vaccines can provide some defense against the infection, the researchers are far away from finding a drug against it [7]. Efforts were directed to repurpose drugs already used for different indications or to find molecules present in the scientific domain with limited toxicity profiles.

Since ancient times, in different traditional health practices, herbs are used as potent therapeutic agents for a plethora of diseases [8,9]. Phytochemicals are an important source of antiviral drugs and reportedly between 1981 and 2006, 44% of approved antiviral drugs originated from plant-derived secondary metabolites. In the plant kingdom, nearly 50,000 secondary metabolites have been reported so far [10,11]. In silico analysis has shown that compounds such as spermidine, spermine, resveratrol, trehalose, baicalin, curcumin, quercetin, epigallocatechin 3-gallate, naringenin, and some flavonoids can act as effective inhibitors of SARS-CoV-2 [12,13]. Terpenoids are a class of plant secondary metabolites formed by the linear arrangement of isoprene units (2-methylbuta-1,3-diene) which might undergo rearrangement and cyclization [14]. Terpenoids have been shown in studies to have potential as SARS-CoV-2 M^{pro} inhibitors [15-18]. Moreover, the potency of terpenoids as antiviral agents can be significantly increased by complexation with metals [19].

Drug repurposing is a promising and exciting strategy that permits the utilization of certain authorized pharmaceutical drugs beyond their intended indication, thereby rendering the options for development of new therapeutics faster. The parallelism in the pathophysiology of COVID-19 and cancer, particularly landmarked by dysfunctional inflammatory and immunologic responses, has driven the endeavors

of repurposing anticancer drugs [20-22]. Plants have been well documented as rich natural source of secondary metabolites with potent in vitro and in vivo anticancer activities [23]; hence, their repurposing as antiviral lead compounds holds great potential. Homalomena aromatica Schott. is a medicinal herb rich in terpenoids, which is used in different traditional health practices of South-East Asia to treat health-related disorders such as inflammation [24], digestive disorders, skin diseases [25], pain, depression, sepsis, spasm, common colds, and insomnia [26]. Therefore, in the present study, a library of terpenoids reported from H. aromatica was initially studied for their binding against SARS-CoV-2 M^{pro} followed by subsequently detailed search in different databases to identify compounds based on the best-docked conformation to identify terpenoid-metal complexes. It was noticed during the search that, thiosemicarbazone complexes showed potent antiviral activity and were found to be significant inhibitors against the human immunodeficiency virus, human T-cell leukemia virus, and herpes simplex virus [27,28]. Subsequently, cuminaldehyde thiosemicarbazone (CT) was taken as a prospective inhibitor of M^{pro} enzyme based on the -CDocker energy of cuminaldehyde [29,30]. In the absence of known inhibitors of SARS-CoV-2 M^{pro}, it was observed by Jin and coworkers that some compounds acted as inhibitors to the enzyme; therefore, the above-mentioned compounds were further analyzed considering the compounds reported by Jin and coworkers including disulfiram (DS), carmofur (CF), ebselen (EL), shikonin (SN), tideglusib (TL), 1-methylpropyl 2-imidazolyl disulfide (PX-12), and 2-methyl-4-(phenylmethyl)-1,2,4-thiadiazolidine-3,5-dione (TDZD-8) [31]. DS was considered for the study on basis of the available literature and the CT inhibition was compared with DS [32-35]. The best-docked compounds namely CT, DS, and the active inhibitor of SARS-CoV-2 M^{pro}, i.e., N3 were further analyzed for binding stability of the top hits by the application of Molecular Dynamics protocol of Discovery Studio 2018. The potential inhibitors for SARS-CoV-2 M^{pro} were identified by the application of different in silico strategies, which are summarized in Scheme 1.

SARS-CoV-2 M^{pro} is an important enzyme for the replication of SARS-CoV-2 as it processes the polyproteins [36] from the viral RNA in the process of translation [37]. Considering the circumstances, and development of recombinant variants like Omicron, it is of utmost importance to find novel molecules since viruses can undergo subtle



Scheme 1: Computational scheme for the identification of inhibitors of SARS-CoV-2 M^{pro} from phytochemicals of *H. aromatica*.

genetic changes through mutation and recombination [38,39]. Additionally, in the case of viruses, alterations in just a handful of amino acid residues in the targeted viral protein are enough to totally or partially negate drug effectiveness [40]. Therefore, on the hunt for novel plant-derived lead anti-SARS-CoV-2 compounds, the current study employed virtual screening and integrated molecular docking approaches to identify secondary metabolites that exhibit promising inhibitory action against its main protease.

2 Results

2.1 Docking study

The redocking of the co-crystalized ligand N3 at the active site gave satisfactory results with an average root mean square value of 2.29 Å. Besides the 2D interactions generated from the original complex and redocked complex also showed reliability of the study with the presence of similar type of non-bond interactions in both cases. The superimposed poses and 2D interaction files are shown Figure S3. The results of the docking analysis for all phytochemicals of H. aromatica are reported in Table S1. Out of the 71 reported molecules from H. aromatica, five molecules were considered based on the -CDocker Energy. Hexadecanoic acid (HM 50) was not considered due to the ADMET profile

of the molecule [41]. The -CDocker Energy of dihydrocuminaldehyde (HM 5), p-cymen-8-ol (HM 37), cuminaldehyde (HM 38), p-cymene (HM 57), and cuminol (HM 65) were found to be significant. N3 complex with M^{pro} was found to be much more stable in comparison with the best hits. Literature suggested that HIS 41 and CYS 148 residues of the protease enzyme of progenitor bat coronavirus that causes MERS are important because of the inhibitory activity of the ligands [42]. After analyzing the interactions of N3, it was observed that N3 interacted with HIS 41 via a hydrophobic bond. On the other hand, HM 5 showed both hydrophilic and hydrophobic interactions with CYS 145. The interaction of HM 37 and HM 57 was analyzed and it was observed that the interaction of both with CYS 145 was hydrophobic. HM 65 showed the formation of a Pi-sulfur bond with CYS145. The detailed interactions of the top hits are summarized in Table 1.

Taking the top hits as the reference structures, a detailed search was performed in different databases to find antiviral molecules. It was observed that CT and para-cymene ruthenium chloride (PCRC) are potent antiviral molecules in vitro [29.30]. CT was considered a significantly better hit against SARS-CoV-2 M^{pro} owing to a better safety profile in association with the -CDocker and binding energies.

The bonding of the amino acids with CT, PCRC, DS, CF, EL, SN, TL, PX-12, and TDZD-8 was found to be hydrophobic. In the docking analysis, it was observed that CF had a binding energy of -65.502 whereas DS showed the highest -CDocker energy. Therefore, DS was considered a

Table 1: ADMET profile of the selected compounds in comparison to the co-crystal ligand

Molecules	ADMET solubility level	ADMET BBB level	ADMET absorption level	CYP2D6	ADMET hepatotoxicity	ADMET PPB level	ADMET AlogP98	ADMET PSA_2D
N3	3	4	3	False	True	False	3.542	206.36
HM 5	3	2	0	False	True	True	2.299	58.931
HM 37	3	1	0	False	False	True	2.294	20.815
HM 38	3	1	0	False	False	True	2.783	17.3
HM 57	3	0	0	False	True	True	3.51	0
HM 65	3	1	0	False	False	True	2.419	20.815
T	3	2	0	False	True	False	2.902	50.673
PCRC	3	1	0	False	True	False	2.641	26.316
OS	2	0	0	False	True	False	4.551	6.704
F	3	3	0	False	True	False	1.844	80.875
iL .	2	1	0	False	True	True	3.227	20.653
SN	3	3	0	False	True	True	2.444	97.048
L	1	0	0	False	True	True	5.155	41.306
X-12	3	1	0	False	True	False	2.641	26.316
DZD-8	3	1	0	False	False	False	2.67	41.306

N3: active inhibitor of SARS-CoV-2 M^{pro}; CT: cuminaldehyde thiosemicarbazone; PCRC: para-cymene ruthenium chloride; DS: disulfiram; CF: carmofur; EL: ebselen; SN: shikonin; TL: tideglusib; PX-12: 1-methylpropyl 2-imidazolyl disulfide; TDZD8: 2-methyl-4-(phenylmethyl)-1,2,4-thiadiazolidine-3,5dione

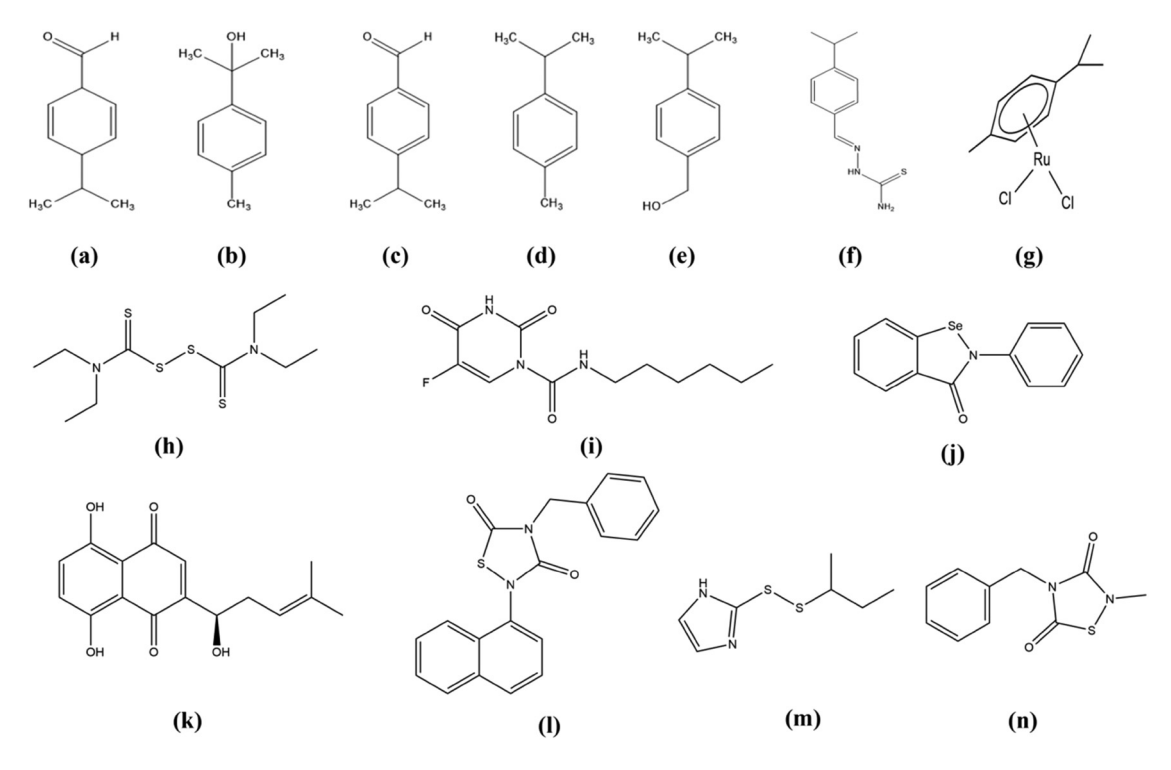


Figure 1: Structure of the best hits: (a) HM 5, (b) HM 37, (c) HM 38, (d) HM 57, (e) HM 65, (f) CT, (g) PCRC, (h) DS, (i) CF, (j) EL, (k) SN, (l) TL, (m) PX-12, and (n) TDZD-8.

better hit of the reference set against SARS-CoV-2 M^{pro}. The 2D structures of the best hits are shown in Figure 1. The results of the docking studies of the top hits are summarized in Table 2. The interacting amino acids for N3, CT, and DS are shown in Figure 2. The 2D interaction of the other molecules is given in Figure S1.

2.2 ADMET analysis

After analyzing the ADMET profile of the reported compounds it was observed that all compounds showed good solubility and absorption in the *in silico* study and very high to medium blood–brain barrier (BBB) penetration.

Table 2: Docking scores of the best compounds in comparison with the co-crystal ligand (N3), DS

Molecules	-CDocker energy	Binding energy	LigScore1	LigScore2	-PLP1	-PLP2	-PMF
HM 5	22.446	-18.989	2.71	4.04	43.88	39.74	35.65
HM 37	21.854	-12.52	0.88	3.14	46.18	44.65	8.76
HM 38	20.016	-33.343	0.99	3.34	45.08	41.12	32.8
HM 57	20.034	-21.288	0.76	3.06	43.66	41.66	3.32
HM 65	22.127	-16.22	1.79	3.67	44.52	43.22	23.56
CT	29.152	-49.759	2.79	4.44	75.44	67.26	28.98
PCRC	28.92	-35.731	0.98	3.43	59.3	57.66	2.69
N3	91.375	-162.285	6.35	5.7	146.55	128.84	35.82
DS	26.621	-36.125	1.13	3.88	45.81	39.92	9.76
CF	19.876	-65.502	2.99	4.27	67.05	52.64	-8.57
EL	5.539	-41.542	2.56	4.49	73.22	68.94	36.83
SN	-0.166	-52.911	3.19	4.14	60.62	60.84	45.56
TL	11.606	-24.24	2.29	4.41	68.03	64.56	27.03
PX-12	13.956	-14.447	1.34	3.49	44.43	43.92	28.98
TDZD-8	20.459	-27.082	1.99	3.94	54.53	49.89	28.94

analysis

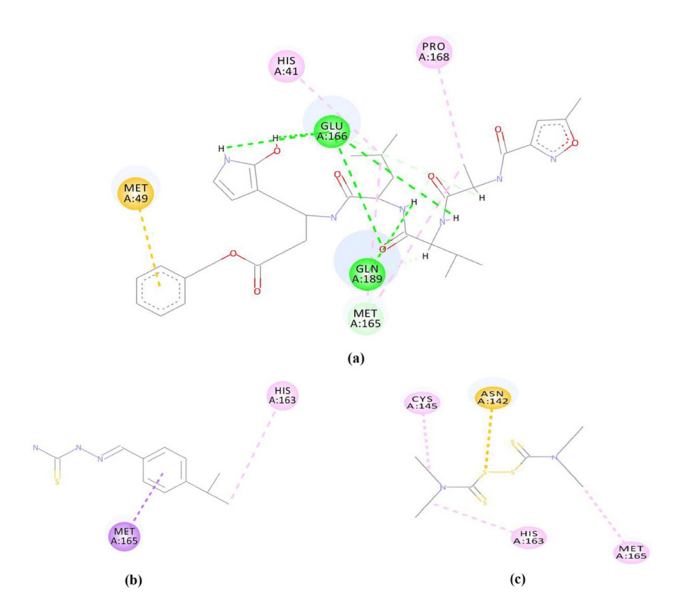


Figure 2: Interactions of M^{pro} with (a) N3, (b) CT, and (c) DS.

Although HM 5 and HM 57 were found to be hepatotoxic, it might also signify that these compounds may not undergo a significant first-pass effect. Nevertheless, all compounds were found to be non-inhibitors of CYP2D6 indicating that each of the reported compounds is metabolized in Phase-I metabolism (Table 3). The toxicity profile of CT was observed to be better than PCRC and was considered a better hit against SARS-CoV-2 M^{pro}. The results of the ADMET analysis are reported in the biplot (Figure 3).

The standard practice in molecular docking calculations

2.3 Molecular dynamics (MD) simulation

involves the assumption that proteins are unchanging or motionless throughout the procedure [43], while the binding of ligand molecules to the receptor displays variability. In order to understand how the drug impacts the energy and mobility of the protein, it is essential for the protein to exhibit smooth movement. The application of MD simulation over a period of 0.5 µs was utilized to enhance our comprehension of the dynamics and visual attributes of the protein [44]. By employing MD simulation, we were able to examine how the protein complex retains its stability, exhibits motion, and undergoes shape modifications over a certain duration. As part of our inquiry, we integrated the root mean square deviation (RMSD) and root-mean-square fluctuation (RMSF) metrics into our analysis, accompanied by a graphical representation illustrating the ligand's interactions with amino acids. Moreover, a comprehensive assessment was carried out to examine the diverse attributes of the ligand. Figures 4-9 display the aforementioned data. Within an acceptable level of deviation, DS was found to be stable in comparison with N3 and CT. The results and findings indicate that the receptor-ligand complexes in all three cases reached a plateau state in less than 5 ns (Figure 4). In the case of N3, the RMSD value reached the plateau and was within 2.5 Å during the period. The RMSD for DS was within 2 Å

Table 3: ADMET prediction of the reported compounds

Molecules	ADMET solubility level	ADMET BBB level	ADMET absorption level	CYP2D6	ADMET hepatotoxicity	ADMET PPB level	ADMET AlogP98	ADMET PSA_2D
N3	3	4	3	False	True	False	3.542	206.36
HM5	3	2	0	False	True	True	2.299	58.931
HM 37	3	1	0	False	False	True	2.294	20.815
HM 38	3	1	0	False	False	True	2.783	17.3
HM 57	3	0	0	False	True	True	3.51	0
HM 65	3	1	0	False	False	True	2.419	20.815
СТ	3	2	0	False	True	False	2.902	50.673
PCRC	3	1	0	False	True	False	2.641	26.316
DS	2	0	0	False	True	False	4.551	6.704
CF	3	3	0	False	True	False	1.844	80.875
EL	2	1	0	False	True	True	3.227	20.653
5N	3	3	0	False	True	True	2.444	97.048
TL	1	0	0	False	True	True	5.155	41.306
PX-12	3	1	0	False	True	False	2.641	26.316
TDZD-8	3	1	0	False	False	False	2.67	41.306

6 — Ashis Kumar Goswami *et al*. DE GRUYTER

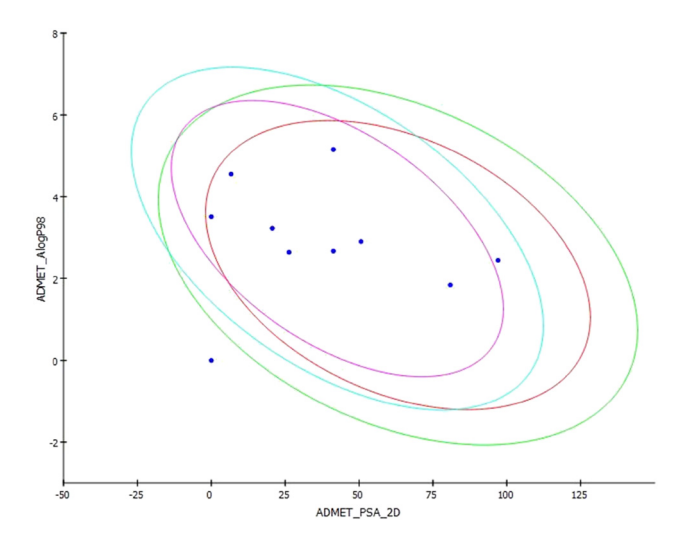


Figure 3: 2D ADMET plot of CT, PCRC, DS, CF, EL, SN, TL, PX-12, and TDZD-8 using a log P98 and PSA_2D.

whereas for CT it was within 2.5 Å. The RMSF plots indicated that the residues in M^{pro} -DS and M^{pro} -CT fluctuated more in comparison with the residues in M^{pro} -N3 (Figure 5).

Figure 6a indicates that strong interactions have been established between the amino acid residues (Leu272, Leu287, Tyr237, and Tyr239) and CT within the protein structure. The most active residues for making interactions with DS are Thr190, Gln192, and Leu167 (Figure 6b). The residues with the highest interactions fraction for N3 are Thr19, Cys21, Ala69, and Thr23 (Figure 6c). Figure 6 also illustrates additional interactions established between the ligands and protein. Figure 7 illustrates the temporal evolution of the number of contacts formed between the ligand and protein, as depicted in the graphical representation. The number of contacts constructed

between N3 and protein is more than those formed between the protein and CT and DS. However, this number for CT is larger than DS. The depiction of the van der Waals surface revealed that the molecular surface area of the substance experienced consistent variations within a limited scope (Figure 8). The solvent-accessible surface area provides a continuous assessment of the interplay between a protein and ligand during their interaction with a solvent (Figure 8). The minor quantity signifies the system's balance. The polar surface area (PSA) is a critical factor in evaluating the molecule's solubility and its ability to dissolve in a solvent (Figure 8). The ability of the solvent to effectively interact with the molecule is directly influenced by the PSA. The assessment is limited to the particular segments of the compound that comprise oxygen and nitrogen atoms. The alteration in the secondary structure elements (SSE) can depict the stability of the protein structure during the simulation. Figure 9 represents the SSE percentage for three simulations and indicates the protein stability during these simulations. As can be seen, the percentage of SSE for CT, DS, and N3 has been at a constant number of about 37.5%, which shows the stability of the protein structure in three simulations.

2.4 Molecular mechanics Poisson–Boltzmann surface area (MM-PBSA)-based binding free energy calculation

The tendency of a substance to bind in the active site of a target protein and the thermodynamic stability of the

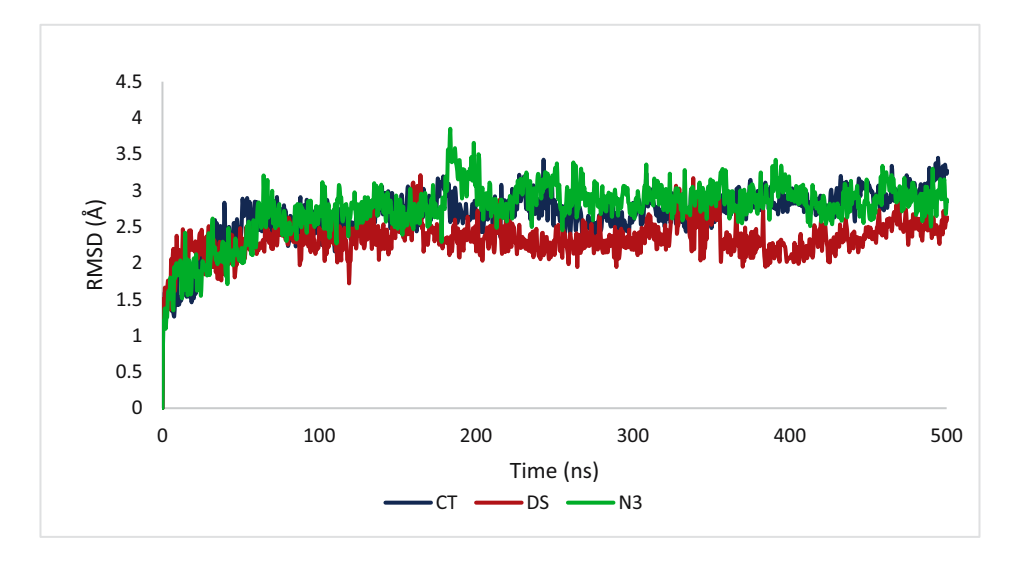


Figure 4: RMSD values of the ligand–protein complexes of CT (blue), DS (red), and N3 (green) during 0.5 μs, which are equilibrated at about 3, 2.5, and 3 Å, respectively.

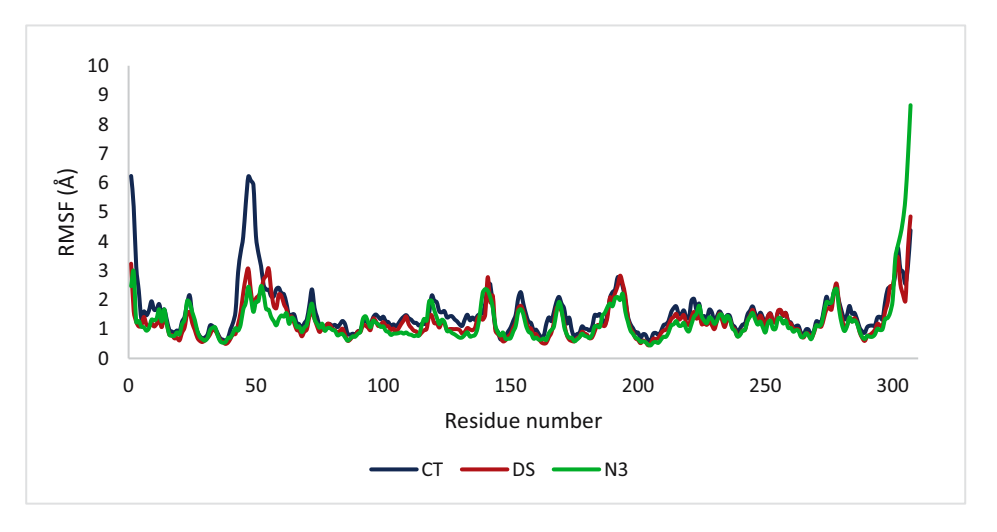


Figure 5: RMSF values of the ligand-protein complexes of CT (blue), DS (red), and N3 (green) during 0.5 µs. The residues in M^{pro}-DS and M^{pro}-CT fluctuated more in comparison with the residues in M^{pro}-N3.

resulting complex are both revealed by the MM-PBSAbased binding free energy. The binding free energies of each conformation produced by the MD simulations were determined in this study, and they were compared to the control complex (M^{pro}-N3) (Figure 7). Finally, the average binding free energies of the three complexes were determined. In the case of M^{pro}-N3 the average binding free energy was -110.021 kcal/mol. But the M^{pro}-DS had higher binding free energy (-33.230 kcal/mol), whereas M^{pro}-CT had lower binding free energy (-169.197 kcal/mol) than M^{pro}-N3. This information suggested that CT would form a thermodynamically stable complex in the binding site of M^{pro}.

3 Discussion

The SARS-CoV-2 pandemic and the SARS and MERS outbreaks is an eye opener that there are no or limited options in front of us to treat this or any zoonotic coronavirus [45]. One of the most interesting sources of therapeutic agents is natural products with their favorable safety and ADME profile, especially for compounds derived from edible plants like H. aromatica. The results revealed that some of the molecules identified from H. aromatica bind with the main protease enzyme of SARS-CoV-2. According to published research, HM 38 exhibits a diverse range of biological action and is reportedly a potent tyrosinase monophenol monooxygenase inhibitor and antiviral agent in vitro [46]. The thiosemicarbazone derivatives are potent anti-microbial agents and showed antibacterial, antiviral, and antitumor activities. Reports also suggested that the bioactivity of molecules increases upon coordination with

metal ions; therefore, it can be inferred that CT will act at a much lesser dose than HM 38 [30]. There are also reported advantages with metal complexes like overcoming resistance developed by microbes against organic molecules which is of utmost importance in designing drugs against viruses that undergo mutation and recombination at a much faster rate [29]. Therefore, CT was selected as a potential antiviral agent against SARS-CoV-2 based on the in silico and ADMET study performed in the present study. Herpes simplex virus type 1 was similarly susceptible to the antiviral effects of HM 57 [47]. Therefore, because of these findings, it is worthy to study the effect of the reported molecules on SARS-CoV-2. It was evident from the MD analysis that CT produced a stable complex in the target's active binding region and interacted with important catalytic residues by forming conventional hydrogen bonds. The MM-PBSA study also suggested that the M^{pro}-CT complex was thermodynamically stable. Since CT formed the complex spontaneously in comparison with the other control complexes, CT could be used as a lead for the development of M^{pro} inhibitors by targeting specific drug development approaches. The screening for the inhibitors of M^{pro} in the study via MD simulations provides important insight for the evaluation of the stability of the docked compounds in the binding pockets even though it is not possible to adequately sample the conformational space owing to the miniature timescale of the study.

4 Materials and methods

The different validated protocols of Discovery Studio 2018 (DS 2018) (Dassault Systèmes BIOVIA, San Diego, USA)

8 — Ashis Kumar Goswami et al. DE GRUYTER

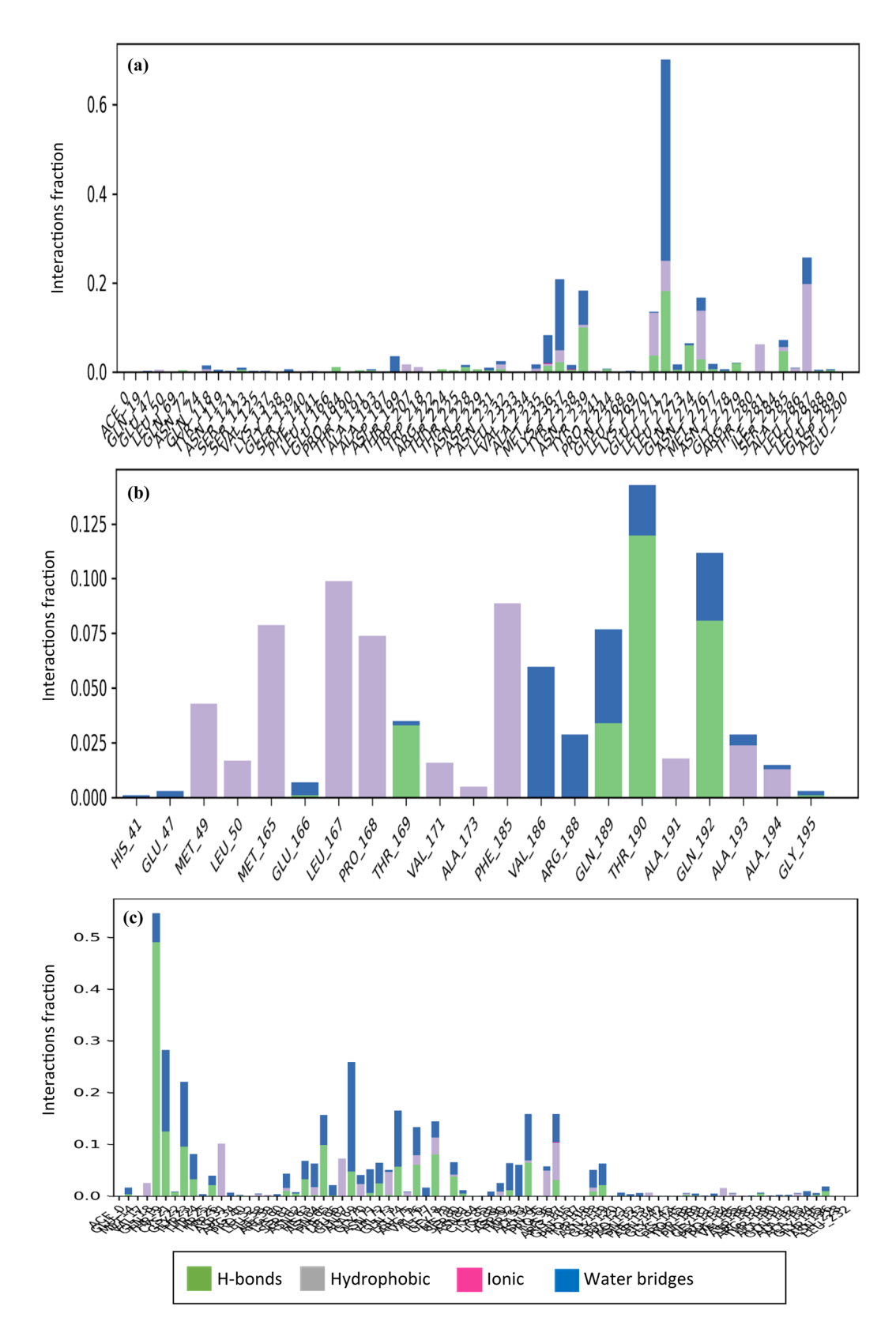


Figure 6: Constructed interactions between the protein structure and the ligands CT (a), DS (b), and N3 (c) during the 0.5 µs MD simulation.

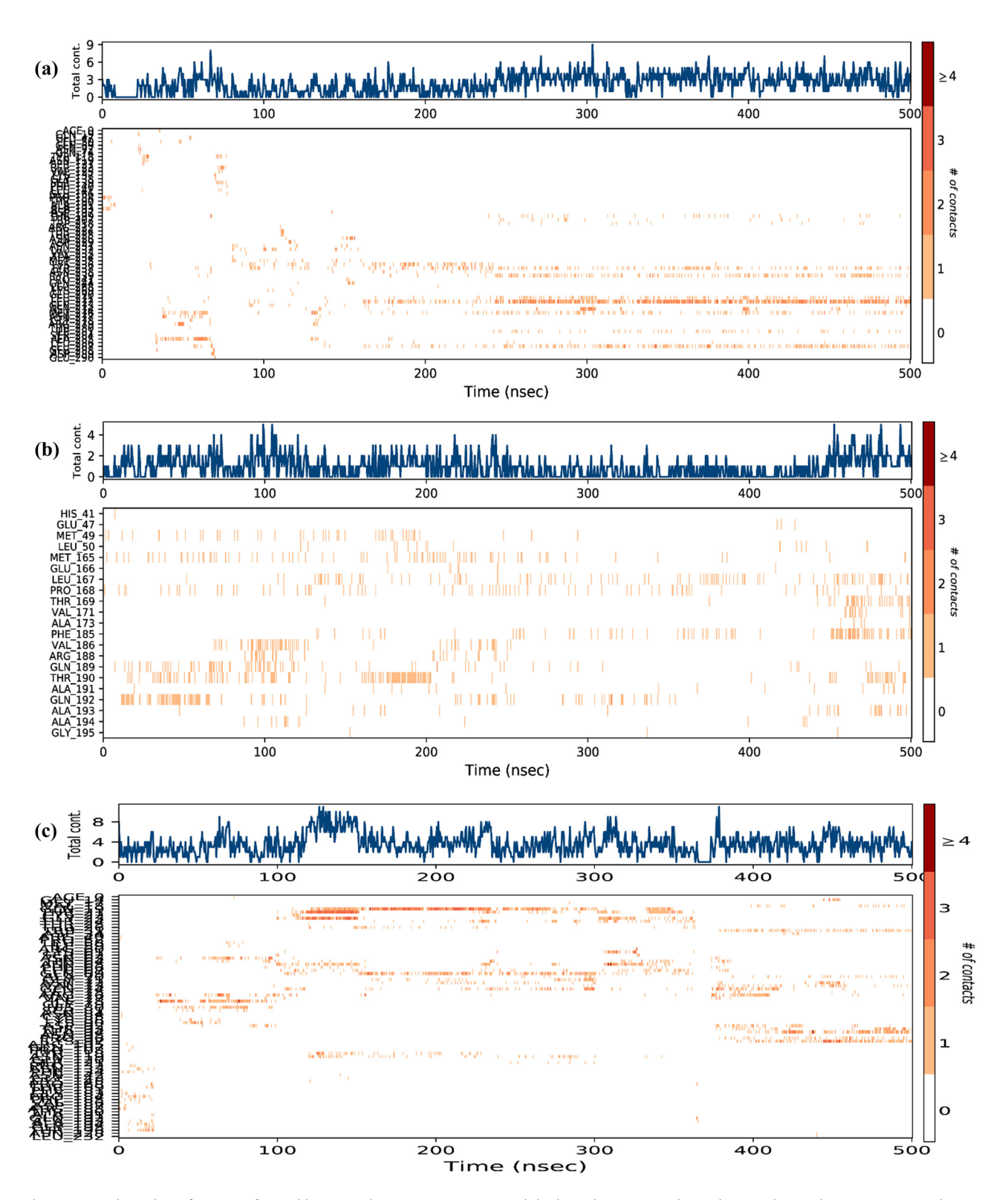


Figure 7: Total number of contacts formed between the protein structure and the ligands CT (a), DS (b), and N3 (c) during the 0.5 µs MD simulation.

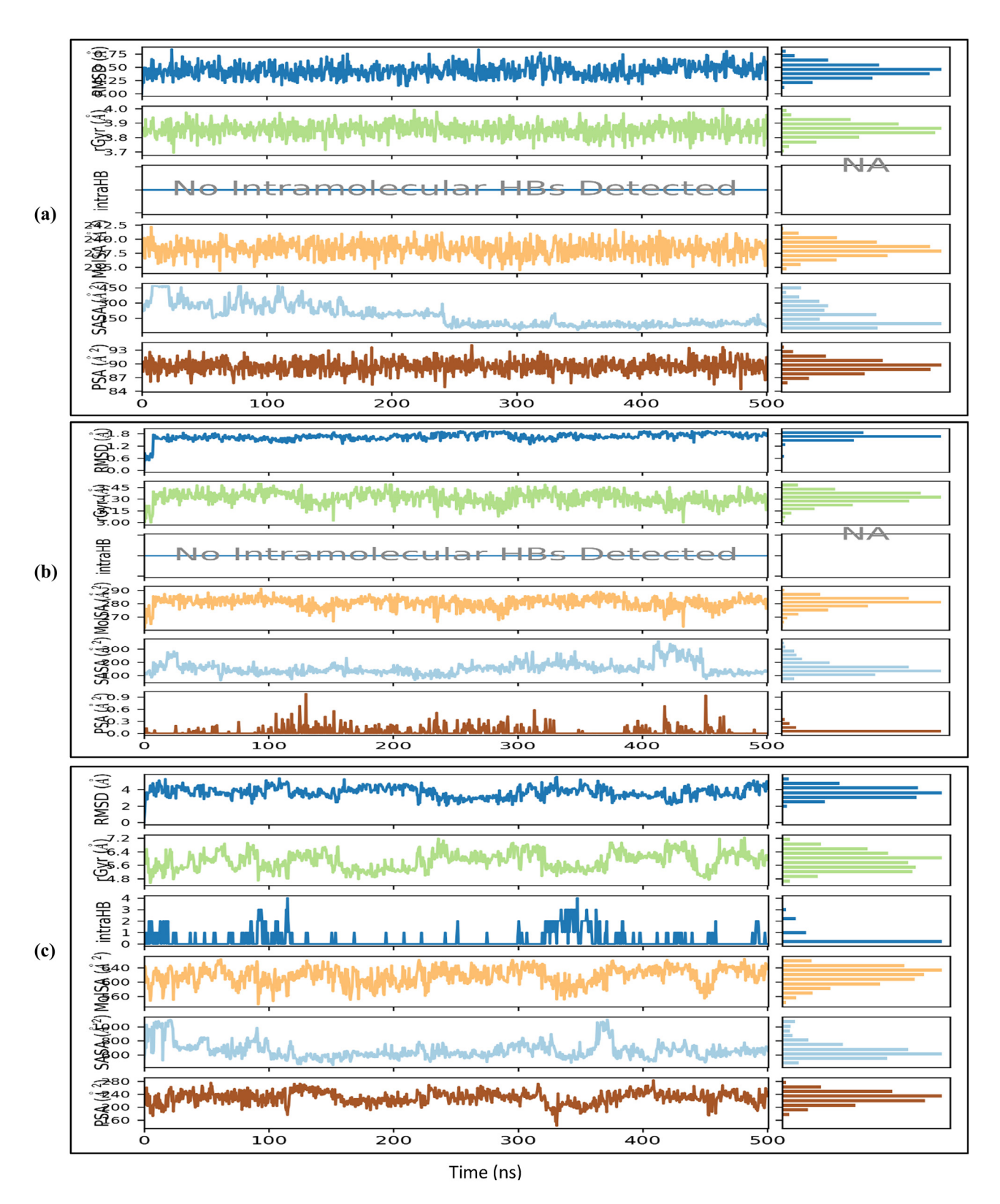


Figure 8: Compound properties of CT (a), DS (b), and N3 (c) during the 0.5 µs MD simulation.

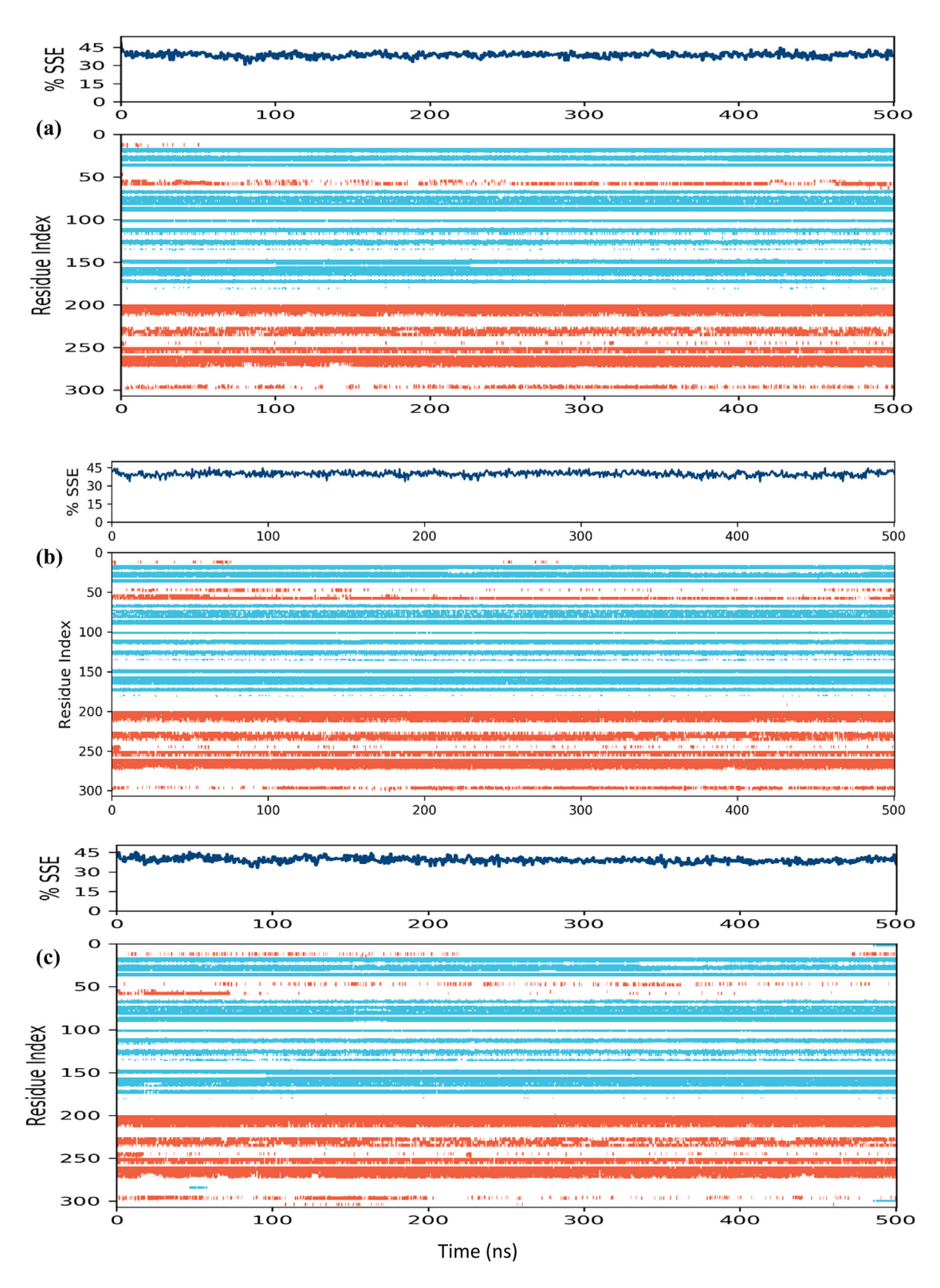


Figure 9: Percentage of SSE for CT (a), DS (b), and N3 (c), which has a constant value of about 37.5% during the 0.5 µs MD simulation.

molecular modeling software was used to perform the computational studies.

selected around the co-crystal ligand N3 with the following co-ordinates: X: -10.897304, Y: 13.066857, Z: 68.557888, and radius: 12.738504 Å (Figure S1).

4.1 Selection of compounds

The compounds were reported as prospective anti-amoebic leads against Entamoeba histolytica in our earlier research work and their in silico toxicity was also ascertained [41]. Taking the best hits from the phytochemicals of *H. aroma*tica as a reference, a detailed search was performed in different databases viz. Pubmed, SciFinder, ChemIDplus, Pub-Chem, DrugBank, Reaxys, Micromedex, Lexi-Comp, Scopus, Phytochemical, Ethnobotanical Databases, Natural Medicines, Google Scholar, and Embase to find antiviral molecules. CT and PCRC were considered for the study after analyzing the different databases [30]. However, DS, CF, EL, SN, TL, PX-12, and TDZD-8 were taken as possible inhibitors of SARS-CoV-2 M^{pro} as reported by Jin et al. [31]. Following the acquisition of the SMILE ids for the molecules from PubChem (www. pubchem.ncbi.nlm.nih.gov), the 3D structures of the molecules were generated. The Chemistry at Harvard Macromolecular Mechanics (CHARMM)-based smart minimizer "Full Minimization" protocol was used to optimize the compounds' energy under the "Small Molecule" tool of Discovery Studio 2018. This protocol uses a Conjugate Gradient algorithm with an energy RMSD gradient of 0.01 kcal/mol, 2,000 steps of steepest descent.

4.2 Preparation of target proteins and validation of the docking protocol

The protein databank website (www.rcsb.org) was accessed and the target protein (PDB ID: 6LU7) was downloaded and loaded to DS 2018. The target protein was cleaned and prepared using the DS 2018 macromolecules tool's "Prepare protein" command (PDB ID: 6LU7). Bond orders and bonds were rectified while the terminal residues were modified. The alternate conformations were deleted during the process of cleaning the target enzyme. The N3 was kept whereas the water molecules were removed during the process. The binding site of N3 was used for the screening of all the molecules. Utilizing the CHARMM-based smart minimizer approach, a perimeter of 200 maximum steps and an energy RMSD gradient of 0.1 kcal/mol were established. The original X-ray crystallographic structure pose of the inhibitor was taken as standard by redocking the active inhibitor for validation of the binding site. The binding site of protein was

4.3 Docking study

The compounds were docked into the active binding site of the target enzyme using the CHARMM-based MD method of the CDocker docking protocol of Discovery Studio 2018. The development of random conformations using high-temperature MD was followed by random rigid-body rotations coupled with simulated annealing to produce conformations of the molecules at the binding site [48,49]. The complex was finally streamlined in order to improve the various postures at the binding site. The binding energies of the best poses were calculated using the Discovery Studio 2018's "Calculate Binding Energy" technique. The molecular binding affinity of the molecules was determined based on LigScore1, LigScore2, piecewise linear potential (-PLP1), piecewise linear potential (-PLP2), and potential of mean force (-PMF). The test results were evaluated wherein the scoring functions of N3 were taken as the control. The structure of M^{pro} with N3 in the active site is given in Figure S2.

4.4 ADMET analysis

The ADMET descriptors algorithm of Discovery Studio 2017 R2 was used to analyze the toxicity profile of each molecule of *H. aromatica* and was previously reported. The different validated protocols of Discovery Studio 2018 (Dassault Systèmes BIOVIA, San Diego, USA) molecular modeling software were used to perform the computational studies. The study's descriptors include aqueous solubility, which forecasts each compound's solubility in water at 25°C, BBB penetration, which anticipates a molecule's penetration of the BBB, CYP2D6 binding, which anticipates the inhibition of the cytochrome P450 2D6 enzyme, hepatotoxicity, which aims to predict dose-dependent human hepatotoxicity, and plasma protein binding. Finally, the absorption level is defined by two parameters namely 2D polar surface area (PSA_2D) and AlogP98, this model has eclipses of 99 and 95% confidence limits that specify the regions for compounds having appropriate intestinal absorption and BBB penetration. The eclipses for the phytochemicals from *H. aromatica* were previously reported by us [12,41,50,51].

These compounds were reported as prospective antiamoebic leads against *E. histolytica* in our earlier research work and their *in silico* toxicity were also ascertained. The ADMET descriptors algorithm of Discovery Studio 2017 R2 was used to analyze the toxicity profile of each molecule of H. aromatica. However, CT, PCRC, DS, CF, EL, SN, TL, PX-12, and TDZD-8 were analyzed for the ADMET descriptors using the "ADMET Descriptors" and "Toxicity Prediction" protocol under the "Small Molecules" tool of the Discovery Studio 2018.

4.5 MD simulations

The effectiveness of protein-compound interactions was evaluated using MD simulation, utilizing Schrödinger's Maestro software, known as Desmond, version 12.8 was utilized to carry out the MD simulation [52], a computational approach operated to investigate dynamic conditions. The complexes of the optimal compounds obtained from the docking investigation (CT, DS, and N3) with COVID-19 main protease (PDB ID: 6LU7) were evaluated dynamically. The simulation was carried out by utilizing the results obtained from the molecular docking process. The MD simulation commenced by utilizing the OPLS force field to reduce the bond energy existing between the proteins and the ligand [53]. The complexes were contained in an orthorhombic container, spaced 10 Å apart, and filled with water [54]. Subsequently, modifications were implemented to the framework through the inclusion of a designated number of Na⁺/Cl⁻ ions. By employing specific measurements for distance, time, temperature, and pressure, the investigation aimed to examine the interaction between chemical compounds and proteins. In the simulation, a cut-off value of 9 Å, a time interval of 2 fs, an initial temperature of 310.15 K (which corresponds to 37°C), and a pressure of 1.01325 bar was utilized [55]. During the examination of Van der Waals and electrostatic interactions, the conservation of these quantities remained unaltered throughout 0.5 µs [56]. The assessment involved the examination of multiple parameters, such as the RMSD, RMSF, the formation of chemical bonds, the characteristics of the ligand, and the SSE.

4.6 MM-PBSA-based binding free energy calculation

One of the crucial parameters to calculate the binding free energy (ΔG) of a substance to a biological macromolecule or target as well as the thermodynamic stability of the protein-ligand complex is the MM-PBSA method [57]. The absolute binding affinity of a chemical within the active binding site of a target protein can be quickly and accurately predicted using this method in the form of binding free energy, which is crucial for the stability and specific potency of the compound [58]. Therefore, using Discovery Studio 2018's "Binding Free Energy - Single Trajectory" protocol and the MM-PBSA method, the binding free energies for each protein-ligand complex were determined following MD simulation. All of the generated conformations' binding free energies were obtained during the study, and each protein-ligand complex's ΔG value was then calculated.

5 Conclusions

The study performed underlines the binding capacity of H. aromatica phytoconstituents revealing that HM 5, HM 37, HM 38, HM 57, and HM 65 exhibit significant binding affinities to the main protease enzyme of SARS-CoV-2. Notably, the binding affinity of CT to M^{pro} of SARS-CoV-2 was found to be higher than all the above-mentioned compounds. However, because of the ever-changing situation concerning COVID-19, it is of utmost importance that researchers and scientists provide important insights into molecules that could result in drug discovery against SARS-CoV-2. These molecules can serve as important prerequisites for quantitative structure-activity relationships to develop anti-SARS-CoV-2 drugs. Further in vitro and in vivo evaluations should be performed for drug candidates in the process of drug discovery against SARS-CoV-2 and its emerging variants. Of particular importance, is the experimental validation of the inhibitory activity of these secondary metabolites against the proposed target enzymes as well other molecular targets such as the spike protein, both in wild and variant viruses, to ascertain their affinities.

Acknowledgements: The authors extend their appreciation to the Deanship of Scientific Research, King Saud University for funding through Vice Deanship of Scientific Research Chairs; COVID-19 Virus Research Chair.

Funding information: The authors extend their appreciation to the Deanship of Scientific Research, King Saud University for funding through Vice Deanship of Scientific Research Chairs; COVID-19 Virus Research Chair.

Author contributions: All authors have contributed equally to conceptualization, execution of the research work, and drafting of the manuscript. All authors have read and agreed to the published version of the manuscript. Ashis Kumar Goswami – data curation, formal analysis, investigation, methodology, writing – original draft preparation; Mourad A. M. Aboul-Soud – investigation, visualization, validation, writing – review & editing; Neelutpal Gogoi – formal analysis, investigation; Mohamed El-Shazly – validation, writing – review & editing; John P. Giesy – visualization, writing – review & editing; Burak Tüzün – methodology, investigation, writing – review & editing; Ibrahim M. Aziz – visualization, validation, writing – review & editing; Fahad N. Almajhdi – data analysis, validation, investigation, funding acquisition, writing – review & editing; Hemanta Kumar Sharma – conceptualization, methodology, supervision, validation, writing – review & editing.

Conflict of interest: The authors declare no conflict of interest.

Ethical approval: The conducted research is not related to either human or animals use.

Data availability statement: The datasets generated during and/or analyzed during the current study are available from the corresponding author on reasonable request.

References

- [1] Battisti V, Wieder O, Garon A, Seidel T, Urban E, Langer T. A computational approach to identify potential novel inhibitors against the coronavirus SARS-CoV-2. Mol Inf. 2020;39:e2000090. doi: 10. 1002/minf.202000090.
- [2] WHO Europe, Coronavirus Disease (COVID-19) Outbreak about the Virus. Available online: http://www.euro.who.int/en/health-topics/ health-emergencies/coronavirus-covid-19/novel-coronavirus-2019ncov (accessed on 23 March 2020).
- [3] WHO, Coronavirus (COVID-19) Events as They Happen. Available online: https://www.who.int/emergencies/diseases/novelcoronavirus-2019/events-as-they-happen (accessed on 23 March 2020).
- [4] Shen M, Zhou Y, Ye J, Abdullah Al-maskri AA, Kang Y, Zeng S, et al. Recent advances and perspectives of nucleic acid detection for coronavirus. J Pharm Anal. 2020;10:97–101. doi: 10.1016/j.jpha.2020. 02.010.
- [5] National Institutes of Health (NIH), Novel Coronavirus Structure Reveals Targets for Vaccines and Treatments. Available online: https://www.nih.gov/news-events/nih-research-matters/novelcoronavirus -structure-reveals- targets-vaccines-treatments (accessed on 17 August 2020).
- [6] Liu S, Zheng Q, Wang Z. Potential covalent drugs targeting the main protease of the SARS-CoV-2 coronavirus. Bioinformatics. 2020;36:3295–8. doi: 10.1093/bioinformatics/btaa224.
- [7] Alves V, Bobrowski T, Melo-Filho C, Korn D, Auerbach S, Schmitt C, et al. QSAR modeling of SARS-CoV M^{pro} inhibitors identifies

- sufugolix, cenicriviroc, proglumetacin and other drugs as candidates for repurposing against SARS-CoV-2. Mol Inf. 2020;40:e2000113. doi: 10.1002/minf.202000113.
- [8] El Gizawy HA, Boshra SA, Mostafa A, Mahmoud SH, Ismail MI, Alsfouk AA, et al. *Pimenta dioica* (L.) Merr. Bioactive constituents exert anti-SARS-CoV-2 and anti-inflammatory activities: Molecular docking and dynamics, *in vitro*, and *in vivo* studies. Molecules. 2021;26:5844. doi: 10.3390/molecules26195844.
- [9] Liang H, Liu H, Kuang Y, Chen L, Ye M, Lai L. Discovery of targeted covalent natural products against PLK1 by herb-based screening. J Chem Inf Model. 2020;60:4350–8. doi: 10.1021/acs.jcim.0c00074.
- [10] Gurung AB, Ali MA, Lee J, Farah MA, Al-Anazi KM. Unravelling lead antiviral phytochemicals for the inhibition of SARS-CoV-2 M^{pro} enzyme through *in silico* approach. Life Sci. 2020;255:117831. doi: 10.1016/j.lfs.2020.117831.
- [11] Anifowose SO, Alqahtani WSN, Al-Dahmash BA, Sasse F, Jalouli M, Aboul-Soud MAM, et al. Efforts in bioprospecting research: a survey of novel anticancer phytochemicals reported in the last decade. Molecules. 2022;27:8307. doi: 10.3390/ MOLECULES27238307.
- [12] Gogoi N, Chowdhury P, Goswami AK, Das A, Chetia D, Gogoi B. Computational guided identification of a citrus flavonoid as potential inhibitor of SARS-CoV-2 main protease. Mol Divers. 2021;25:1745–59. doi: 10.1007/s11030-020-10150-x.
- [13] Khan N, Chen X, Geiger JD. Possible therapeutic use of natural compounds against COVID-19. J Cell Signal. 2021;2:63–79. doi: 10.33696/signaling.2.036.
- [14] Ludwiczuk A, Skalicka-Woźniak K, Georgiev MI. Terpenoids. In: Badal S, Delgoda R, editors. Pharmacognosy fundamentals, applications and strategies. United States: Academic Press; 2017. p. 233–66. doi: 10.1016/B978-0-12-802104-0.00011-1.
- [15] Giofrè SV, Napoli E, Iraci N, Speciale A, Cimino F, Muscarà C, et al. Interaction of selected terpenoids with two SARS-CoV-2 key therapeutic targets: An in silico study through molecular docking and dynamics simulations. Comput Biol Med. 2021;134:104538. doi: 10.1016/J.COMPBIOMED.2021.104538.
- [16] Gyebi GA, Ogunro OB, Adegunloye AP, Ogunyemi OM, Afolabi SO. Potential inhibitors of coronavirus 3-chymotrypsin-like protease (3CLpro): An *in silico* screening of alkaloids and terpenoids from African medicinal plants. J Biomol Struct Dyn. 2020;39:3396–408. doi: 10.1080/07391102 .2020.1764868.
- [17] Sepay N, Sekar A, Halder UC, Alarifi A, Afzal M. Anti-COVID-19 terpenoid from marine sources: A docking, ADMET and molecular dynamics study. J Mol Struct. 2021;1228:129433. doi: 10.1016/J. MOLSTRUC.2020.129433.
- [18] Boozari M, Hosseinzadeh H. Natural products for COVID-19 prevention and treatment regarding to previous coronavirus infections and novel studies. Phyther Res. 2021;35:864–76. doi: 10.1002/PTR.6873.
- [19] Wen CC, Kuo YH, Jan JT, Liang PH, Wang SY, Liu HG, et al. Specific plant terpenoids and lignoids possess potent antiviral activities against severe acute respiratory syndrome coronavirus. J Med Chem. 2007;50:4087–95. doi: 10.1021/JM070295S/ASSET/IMAGES/ MEDIUM/JM070295SN00001.GIF.
- [20] Mahmoud AM, Aboul-Soud MAM, Han J, Al-Sheikh YA, Al-Abd AM, El-Shemy HA. Transcriptional profiling of breast cancer cells in response to mevinolin: Evidence of cell cycle arrest, DNA degradation and apoptosis. Int J Oncol. 2016;48:1886. doi: 10.3892/IJO.2016.3418.
- 21] Aboul-Soud MAM, El-Shemy HA, Aboul-Enein KM, Mahmoud AM, Al-Abd AM, Lightfoot DA. Effects of plant-derived anti-leukemic

- drugs on individualized leukemic cell population profiles in Egyptian patients. Oncol Lett. 2016;11:642-8. doi: 10.3892/OL. 2015.3916.
- [22] El-Shemy H, Aboul-Soud M, Nassr-Allah A, Aboul-Enein K, Kabash A, Yagi A. Antitumor properties and modulation of antioxidant enzymes' activity by Aloe vera leaf active principles isolated via supercritical carbon dioxide extraction. Curr Med Chem. 2010:17:129-38. doi: 10.2174/092986710790112620.
- [23] Aldea M, Michot JM, Danlos FX, Ribas A, Soria JC. Repurposing of anticancer drugs expands possibilities for antiviral and antiinflammatory discovery in COVID-19. Cancer Discovery. 2021;11:1336-44. doi: 10.1158/2159-8290.cd-21-0144/673855/am/ repurposing-of-anticancer-drugs-expands.
- [24] Majumdar K, Datta BK. A study on ethnomedicinal usage of plants among the folklore herbalists and tripuri medical practitioners: Part-II. Nat Prod Radiance. 2016;6:66-73.
- [25] Laishram SKS, Nath DR, Bailung B, Baruah I. In vitro antibacterial activity of essential oil from rhizome of Homalomena aromatica against pathogenic bacteria. J Cell Tissue Res. 2006;6:849-51.
- [26] Policegoudra RS, Goswami S, Aradhya SM, Chatterjee S, Datta S, Sivaswamy R, et al. Bioactive constituents of Homalomena aromatica essential oil and its antifungal activity against dermatophytes and yeasts. J Mycol Med. 2012;22:83-7. doi: 10.1016/j.mycmed.2011. 10.007.
- [27] Pelosi G, Bisceglie F, Bignami F, Ronzi P, Schiavone P, Re MC, et al. Antiretroviral activity of thiosemicarbazone metal complexes. J Med Chem. 2010;53:8765-9. doi: 10.1021/jm1007616.
- [28] Pelosi G. Thiosemicarbazone metal complexes: From structure to activity. Open Crystallogr J. 2010;3:16-28. doi: 10.2174/ 1874846501003020016.
- [29] Allardyce CS, Dyson PJ, Ellis DJ, Salter PA, Scopelliti R. Synthesis and characterisation of some water soluble ruthenium(II)-arene complexes and an investigation of their antibiotic and antiviral properties. J Organomet Chem. 2003;668:35-42. doi: 10.1016/S0022-328X(02)01926-5.
- [30] Bisceglie F, Pinelli S, Alinovi R, Goldoni M, Mutti A, Camerini A, et al. Cinnamaldehyde and cuminaldehyde thiosemicarbazones and their copper(II) and nickel(II) complexes: A study to understand their biological activity. | Inorg Biochem. 2014;140:111-25. doi: 10. 1016/i.iinorabio.2014.07.014.
- [31] Jin Z, Du X, Xu Y, Deng Y, Liu M, Zhao Y, et al. Structure of M^{pro} from SARS-CoV-2 and discovery of its inhibitors. Nature. 2020;582:289-93. doi: 10.1038/s41586-020-2223-y.
- [32] Ma C, Hu Y, Townsend JA, Lagarias PI, Marty MT, Kolocouris A, et al. Ebselen, disulfiram, carmofur, PX-12, tideglusib, and shikonin are nonspecific promiscuous SARS-CoV-2 main protease inhibitors. ACS Pharmacol Transl Sci. 2020;3:1265-77. doi: 10.1021/ACSPTSCI. 0C00130/ASSET/IMAGES/MEDIUM/PT0C00130_0007.GIF.
- [33] Stroylov VS, Svitanko IV. Computational identification of disulfiram and neratinib as putative SARS-CoV-2 main protease inhibitors. Mendeleev Commun. 2020;30:419-20. doi: 10.1016/J.MENCOM. 2020.07.004.
- [34] Xu L, Tong J, Wu Y, Zhao S, Lin BL. A computational evaluation of targeted oxidation strategy (TOS) for potential inhibition of SARS-CoV-2 by disulfiram and analogues. Biophys Chem. 2021;276:106610. doi: 10.1016/J.BPC.2021.106610.
- [35] Singh N, Villoutreix BO. Resources and computational strategies to advance small molecule SARS-CoV-2 discovery: Lessons from the pandemic and preparing for future health crises. Comput Struct Biotechnol J. 2021;19:2537-48. doi: 10.1016/J.CSBJ.2021.04.059.

- [36] Ngo ST, Quynh Anh Pham N, Thi Le L, Pham D-H, Vu VV. Computational determination of potential inhibitors of SARS-CoV-2 main protease. J Chem Inf Model. 2020;60:5771-80. doi: 10.1021/ acs.jcim.0c00491.
- [37] Zhang L, Lin D, Sun X, Curth U, Drosten C, Sauerhering L, et al. Crystal structure of SARS-CoV-2 main protease provides a basis for design of improved α-ketoamide inhibitors. Science. 2020:368:409-12. doi: 10.1126/science.abb3405.
- Dhawan M, Saied ARA, Mitra S, Alhumaydhi FA, Emran TB, [38] Wilairatana P, et al. Omicron variant (B.1.1.529) and its sublineages: What do we know so far amid the emergence of recombinant variants of SARS-CoV-2? Biomed Pharmacother. 2022;154:113522. doi: 10.1016/J.BIOPHA.2022.113522.
- [39] Wimmer E. Goldbach R. Viral genetics, Curr Opin Genet Dev. 1992;2:59-60. doi: 10.1016/S0959-437X(05)80322-3.
- [40] Warfield KL, Schaaf KR, DeWald LE, Spurgers KB, Wang W, Stavale E, et al. Lack of selective resistance of influenza A virus in presence of host-targeted antiviral, UV-4B. Sci Rep. 2019;9:1–13. doi: 10.1038/s41598-019-43030-y.
- Goswami AK, Gogoi N, Gogoi BJ, Sharma HK. Network-Pharmacology and DFT based approach towards identification of leads from Homalomena aromatica for multi-target in-silico screening on Entamoeba histolytica proteins. Curr Drug Ther. 2020;15:226-37. doi: 10.2174/1574885514666190801102336.
- St. John SE, Tomar S, Stauffer SR, Mesecar AD. Targeting zoonotic viruses: Structure-based inhibition of the 3C-like protease from bat coronavirus HKU4 - the likely reservoir host to the human coronavirus that causes middle east respiratory syndrome (MERS). Bioorg Med Chem. 2015;23:6036-48. doi: 10.1016/j.bmc.2015.06.039.
- Poustforoosh A, Faramarz S, Nematollahi MH, Mahmoodi M, Azadpour M. Correction: Structure-based drug design for targeting IRE1: An in silico approach for treatment of cancer. Drug Res. 2024;74:e1. doi: 10.1055/A-2235-8845.
- Poustforoosh A, Faramarz S, Negahdaripour M, Hashemipour H. Modeling and affinity maturation of an anti-CD20 nanobody: a comprehensive in-silico investigation. Sci Rep. 2023;13:582. doi: 10.1038/S41598-023-27926-4.
- [45] Wu C, Liu Y, Yang Y, Zhang P, Zhong W, Wang Y, et al. Analysis of therapeutic targets for SARS-CoV-2 and discovery of potential drugs by computational methods. Acta Pharm Sin B. 2020;10:766-88. doi: 10.1016/j.apsb.2020.02.008.
- [46] Azeez SC. In: Parthasarathy VA, Chempakam B, Zachariah TJ, editors. Chemistry of spices. Oxfordshire: CABI; 2008. p. 211-26.
- Astani A, Reichling J, Schnitzler P. Comparative study on the antiviral activity of selected monoterpenes derived from essential oils. Phyther Res. 2009;24:673-9. doi: 10.1002/ptr.2955.
- [48] Kumar A, Alfhili MA, Bari A, Ennaji H, Ahamed M, Bourhia M, et al. Apoptosis-mediated anti-proliferative activity of Calligonum comosum against human breast cancer cells, and molecular docking of its major polyphenolics to caspase-3. Front Cell Dev Biol. 2022;10:972111. doi: 10.3389/FCELL.2022.972111.
- Aboul-Soud MAM, Ennaji H, Kumar A, Alfhili MA, Bari A, Ahamed M, et al. Antioxidant, anti-proliferative activity and chemical fingerprinting of Centaurea calcitrapa against breast cancer cells and molecular docking of caspase-3. Antioxidants. 2022;11:1514. doi: 10. 3390/ANTIOX11081514.
- Gogoi N, Chowdhury P, Goswami AK, Das A, Chetia D, Gogoi B. Integrated computational approach towards repurposing of antimalarial drug against SARS-CoV-2 main protease. Struct Chem. 2022;33:1409-22. doi: 10.1007/s11224-022-01916-0.

- [51] Goswami AK, Sharma HK, Gogoi N, Kashyap A, Gogoi BJ. *In vitro* evaluation and molecular dynamics, DFT guided investigation of antimalarial activity of ethnomedicinally used *Coptis teeta* wall. Comb Chem High Throughput Screening. 2021;25:292–306. doi: 10. 2174/1386207324666210118095503.
- [52] Bowers KJ, Chow DE, Xu H, Dror RO, Eastwood MP, Gregersen BA, et al. Scalable algorithms for molecular dynamics simulations on commodity clusters. In Proceedings of the ACM/IEEE SC 2006 Conference (SC'06). IEEE; 2006. p. 43–3.
- [53] Poustforoosh A, Moosavi F. Evaluation of the FDA-approved kinase inhibitors to uncover the potential repurposing candidates targeting ABC transporters in multidrug-resistant cancer cells: an in silico approach. J Biomol Struct Dyn. 2023;1–13. doi: 10.1080/ 07391102.2023.2277848.
- [54] Poustforoosh A, Faramarz S, Negahdaripour M, Tüzün B, Hashemipour H. Investigation on the mechanisms by which the herbal remedies induce anti-prostate cancer activity: Uncovering the most practical natural compound.

- J Biomol Struct Dyn. 2024;42:3349–62. doi: 10.1080/07391102.2023. 2213344.
- [55] Poustforoosh A. Investigation on the structural and dynamical properties of cationic, anionic, and catanionic niosomes as multifunctional controlled drug delivery system for cabozantinib. Colloids Surf, A. 2024;687:133547. doi: 10.1016/J.COLSURFA.2024. 133547.
- [56] Poustforoosh A, Faramarz S, Negahdaripour M, Tüzün B, Hashemipour H. Tracing the pathways and mechanisms involved in the anti-breast cancer activity of glycyrrhizin using bioinformatics tools and computational methods. J Biomol Struct Dyn. 2024;42:819–33. doi: 10.1080/07391102.2023.2196347.
- [57] Genheden S, Ryde U. The MM/PBSA and MM/GBSA methods to estimate ligand-binding affinities. Expert Opin Drug Discov. 2015;10:449–61. doi: 10.1517/17460441.2015.1032936.
- [58] Rastelli G, Del Rio A, Degliesposti G, Sgobba M. Fast and accurate predictions of binding free energies using MM-PBSA and MM-GBSA. J Comput Chem. 2010;31:797–810. doi: 10.1002/jcc.21372.